HHS Public Access

Author manuscript

Photochem Photobiol. Author manuscript; available in PMC 2016 January 08.

Published in final edited form as:

Photochem Photobiol. 2014 ; 90(2): 306–312. doi:10.1111/php.12226.

Chemosensitization of Cancer Cells via Gold Nanoparticle-Induced Cell Cycle Regulation

Megan A. Mackey and **Mostafa A. El-Sayed***

Laser Dynamics Laboratory, School of Chemistry and Biochemistry, Georgia Institute of Technology, Atlanta, Georgia, USA

Abstract

We have previously shown that plasmonic nanoparticles conjugated with nuclear-targeting and cytoplasm-targeting peptides (NLS and RGD, respectively) are capable of altering the cell cycle of human oral squamous carcinoma cells (HSC-3). In the present work, we show that this regulation of the cell cycle can be exploited to enhance the efficacy of a common chemotherapeutic agent, 5-Fluorouracil, by pre-treating cells with gold nanoparticles. Utilizing flow cytometry cell cycle analysis, we were able to quantify the 5-Fluorouracil efficacy as an accumulation of cells in the S phase with a depletion of cells in the G2/M phase. Two gold nanoparticle sizes were tested in this work; 30 nm with a surface plasmon resonance at 530 nm and 15 nm with a surface plasmon resonance at 520 nm. The 30 nm nuclear-targeted gold nanoparticles (NLS-AuNPs) showed the greatest 5-Fluorouracil efficacy enhancement when 5-Fluorouracil treatment (500 μM, 48 h) is preceded by a 24 h treatment with nanoparticles. In conclusion, we show that nuclear-targeted 30 nm gold nanoparticles enhance 5-Fluorouracil drug efficacy in HSC-3 cells via regulation of the cell cycle, a chemosensitization technique that could potentially be expanded to different cell lines and different chemotherapies.

INTRODUCTION

Noble metal nanoparticles are becoming increasingly prominent in the treatment of disease due to their unique properties as both intrinsic antineoplastic agents(1–4) and extrinsic photothermal contrast agents.(5–11) Gold nanoparticles, in particular, are showing great promise as antineoplastic agents, especially with their ability to prohibit cell growth and regulate the cell cycle without external stimulation via radiation.(2, 4, 12–14) Specifically, cell cycle regulation by gold nanoparticles has been utilized for the sensitization of malignant cells to radiation. For example, Roa, et al.(14) previously showed that glucose-capped gold nanoparticles caused accumulation of prostate cancer cells (DU145) in the G2/M phase of the cell cycle and subsequent radiation sensitization of these cells, as cells in the G2/M phase are most vulnerable to radiation. Another group later showed that peptide-capped gold nanorods were capable of sensitizing melanoma cells (A375) to radiation, also through a G2/M arrest.(15)

*Corresponding author: Mostafa A. El-Sayed, 901 Atlantic Drive, Atlanta, Georgia, 30332-0400, USA. phone: 404-894-0292, fax: 404-894-7452, melsayed@gatech.edu.

Cell cycle regulation by gold nanoparticles could also potentially be useful for sensitization of malignant cell lines to chemotherapeutic agents. For example, the antimetabolite drug 5-Fluorouracil (5-FU) specifically acts on cells present in the S phase of the cell cycle.(16) Additionally, a population of cells is resistant to 5-FU treatment when there is a depletion of cells in the S phase with an accumulation of cells in the G2/M phase.(17, 18) With the extensive research done on the use of 5-FU as a chemotherapeutic agent and its mode of action, it is possible to now enhance 5-FU chemosensitivity in cells, namely by regulating the cell cycle.

In the present work, we show that gold nanoparticles, specifically conjugated with nuclear-targeting peptides, are capable of regulating the cell cycle, such that they induce an S phase accumulation and G2/M phase depletion. Subsequently, these gold nanoparticles enhance the chemosensitivity of a human oral squamous carcinoma cell line to 5-FU treatment, as shown by a cell viability assay. Along with the cell viability results, the mode of cell death is assessed by flow cytometry analysis of apoptotic and necrotic cells. With these results, it is again apparent that the pre-treatment of cells with nuclear-targeting gold nanoparticles, can enhance cell death pathways characteristic of 5-FU treatment. The cell cycle regulation and subsequent enhancement of 5-FU efficacy seen with the gold nanoparticles investigated in this work is dependent upon both nanoparticle size and nanoparticle functionalization (*i.e.* location of nanoparticles within cells). Also interesting is that the gold nanoparticles are not inherently cytotoxic to the cells, potentially minimizing toxicity issues commonly presented with combination chemotherapies.

MATERIALS AND METHODS

Cell Culture

Human oral squamous cell carcinoma (HSC-3) cells were maintained in Dulbecco's modified Eagle's medium (DMEM, Mediatech) supplemented with 10% v/v fetal bovine serum (FBS, Mediatech) and 1% v/v antimycotic solution (Mediatech) in a 37°C, 5% CO_2 humidified incubator.

Gold Nanoparticle Synthesis and Peptide Conjugation

Gold nanoparticles (AuNPs) were synthesized via citrate reduction of chloroauric acid ($HAuCl_4$), as developed by Frens(19) Briefly, 50 mL of a 0.01% (w/v) $HAuCl_4$ aqueous solution is brought to a boil, while stirring, followed by addition of a trisodium citrate aqueous solution. The reaction is determined to reach completion when the solution color changes from clear to a deep red/purple. To obtain AuNPs with a 30 nm diameter and a surface plasmon resonance at 530 nm (Fig. 1A), 1 mL of 1% (w/v) trisodium citrate was added to the $HAuCl_4$ solution. To obtain AuNPs with a 15 nm diameter and a surface plasmon resonance at 520 nm (Fig. 1B), 1 mL of 2% trisodium citrate (w/v) was added. The AuNPs were then purified by centrifugation at 6000 rpm for 15 min and redispersed in water. The core nanoparticle diameters were determined using ImageJ software. Extinction coefficients used for the 30 and 15 nm AuNPs (3.0×10^9 and 3.6×10^8 $M^{-1}cm^{-1}$, respectively) were based on previous reports.(20)

The as-synthesized AuNPs are first stabilized with polyethylene glycol (mPEG-SH, MW 5000, Laysan Bio, Inc.) to prevent nonspecific adsorption of proteins and other biological components in the physiological environment. Stabilization with PEG was achieved through addition of a 1 mM aqueous solution of PEG to the AuNP solution at a molar excess of 10^4 and shaking on an orbital shaker overnight at room temperature. After PEG stabilization, the AuNPs were centrifuged at 6000 rpm for 15 min and redispersed in water.

The now PEG-stabilized AuNPs were functionalized with custom peptides purchased from GenScript USA, Inc, as we have previously demonstrated.(4) Specifically, an NLS (nuclear localization sequence) peptide with the sequence CGGGPKKKRKVGG and an RGD (Arg-Gly-Asp) peptide with the sequence $(RGD)_4$ PGC were used throughout this work. Peptide conjugation was achieved through addition of a 5 mM aqueous solution of peptides to the PEG-AuNP solutions at a molar excess of 10^4 and shaking on an orbital shaker overnight at room temperature. The peptide-conjugated AuNPs were then purified by centrifugation at 6000 rpm for 15 min and redispersed in water. Three different nanoparticle formulations were utilized in this study; 15 nm NLS-AuNPs, 30 nm NLS-AuNPs and 30 nm RGD-AuNPs.

In order to confirm nanoparticle functionalization, the hydrodynamic diameter (HD) and zeta potential were measured via dynamic light scattering (DLS). Table 1 displays the increasing HD and neutralization of zeta potential upon conjugation of citrate-capped AuNPs with PEG and peptides.

Treatment of Cells with AuNPs and 5-Fluorouracil

HSC-3 cells were treated with both AuNPs and 5-Fluorouracil (5-FU). Briefly, after cells were grown overnight, a 0.4 nM concentration of AuNPs (in cell culture medium) was added to the cells. Cells were treated with AuNPs for 24 h, after which, they were washed with PBS and subsequently treated with various concentrations of 5-FU. Cells were treated with 5-FU for 48 h before performing analyses. The control samples in this work are treated with an appropriate concentration of DMSO in cell culture medium (0.2%) corresponding to the highest percentage of DMSO that is introduced to cells by the 5-FU treatment.

Flow Cytometry Cell Cycle Analysis

In order to determine the percentages of cells that exist in specific phases of the cell cycle, flow cytometry cell cycle analysis was performed. Briefly, HSC cells were plated in a 12-well tissue culture plate. Cells were allowed to grow overnight after which treatment was administered according to method described above. Upon treatment of cells, they are washed with PBS, collected by trypsinization and centrifugation, and fixed in 70% ice cold ethanol and storage at −20 °C. For preparation of cells for flow cytometry cell cycle analysis, the fixed cell suspension is centrifuged and a cell pellet is obtained. The cells are then redispersed in PBS (750 uL) and 5 uL of 2 mg/mL RNase is added and the cells are incubated at 37 °C for 30 min. After RNase treatment, cells are stained with 75 uL of the fluorescent nucleic acid dye, Propidium iodide (PI, 1 mg/mL). Cells are then incubated at room temperature for 15 min, after which they are passed through a 40 um sterile filter. Cells are then analyzed on a BD LSR II (BD Biosciences) with a 488 nm excitation. Flow

cytometry data is analyzed using the flow cytometry analysis software, FlowJo. Results are reported as the average % of cells in each phase of the cell cycle ± standard deviation.

Cell Viability Assay

In order to determine cell viability, an XTT assay (Biotium, Inc. Cat# 30007) was utilized. Briefly, HSC cells were plated in a 96-well tissue culture plate. Cells were allowed to grow overnight, after which, treatment was administered according to method described above. Upon treatment of cells, they are washed with PBS and then incubated with the activated XTT reagent (prepared according to manufacturer's protocol) for 5 h. The cell viability is determined based on spectrophotometric measurements of the XTT reagent with a Biotek Synergy H4 multi-mode plate reader. All treated groups are normalized to the control (HSC cells treated with 0.2% DMSO) and results are reported as the average % viability ± % relative standard deviation.

Apoptosis and Necrosis Detection via Flow Cytometry

In order to quantify the various modes of cell death that are potentially involved with the combination treatment of AuNPs and 5-FU, the *ApoTarget*™ Annexin-V FITC Apoptosis Kit (Invitrogen, Inc. Cat. #PHN1010) was utilized. The standard protocol was optimized for our experimental conditions. Briefly, HSC cells were plated in a 12-well tissue culture plate. Cells were allowed to grow overnight after which treatment was administered according to method described above. Upon treatment of cells, they are washed with PBS and collected by trypsinization and centrifugation. The cells are then washed again with cold PBS and collected by centrifugation, after which, 500 μL of 1x Annexin binding buffer, 2 μL of 100 μg/mL PI and 5 μL of Annexin-V-FITC are all mixed with the cells and left to incubate for 15 min at room temperature. Following cell staining with PI and Annexin-V-FITC, the remaining volume of 1x Annexin binding buffer was added (493 μL) and the cell solution was passed through a 40 μm sterile filter. Cells are then analyzed on a BD LSR II (BD Biosciences) with a 488 nm excitation. Flow cytometry data is analyzed using the flow cytometry analysis software, FlowJo. Results are reported as the average % of cells in each phase of the cell cycle ± standard deviation.

Statistical Analysis

Statistical significance was determined with the *t test calculator* (GraphPad Software, Inc.). Data is considered statistically significant when $p < 0.05$ and is indicated by *.

RESULTS AND DISCUSSION

Gold Nanoparticle Induced Cell Cycle Regulation

Cell cycle regulation can be advantageous, specifically for the sensitization of malignant cells to specific methods of cancer treatment.(14, 15) Particularly, some chemotherapeutic agents act on cells that are in a specific phase of the cell cycle (*e.g.* G0/G1, S, or G2/M). For example, 5-Fluorouracil (5-FU), a standard drug utilized in the clinical treatment of cancers of the head and neck,(21, 22) is most effective when cells are in the S phase of the cell cycle, as it is associated with the incorporation of fluoronucleotides (*e.g.* fluorodeoxyuridine triphosphate, FdUTP) in place of nucleotides (*e.g.* deoxyuridine triphosphate, dUTP) in the

cell's RNA.(16–18) Since we have shown previously that AuNPs conjugated with NLS and RGD peptides have the ability to alter the cell cycle of HSC-3 cells(2, 4), we took this further by testing their ability to chemosensitize HSC-3 cells to 5-FU treatment *in vitro*. In order to first estimate the efficacy by which these nanoparticles chemosensitize HSC-3 cells to 5-FU treatment, we performed cell cycle analysis on cells after a 24 h treatment with various AuNPs (0.4 nM), as well as a subsequent treatment with 100 μM 5-FU. In order to compare cell cycle regulation between nanoparticle size, 15 and 30 nm NLS-AuNPs, known to localize at the nucleus of HSC-3 cells,(4) were tested. In order to compare between the location of nanoparticles within cells (*i.e.* AuNP surface functionalization), the 30 nm NLS-AuNPs were also compared to RGD-AuNPs, known to localize in the cytoplasm of HSC-3 cells.(4) Figure 2 shows the cell cycle analysis of HSC-3 cells after various treatments. Interesting here is that all nanoparticles induce an increase in the S phase population and a decrease in the G2/M phase population of cells after a 24 h treatment. Also shown in the cell cycle analysis is that 100 μM 5-FU itself induces an S phase accumulation with a G2/M phase depletion. The combination treatment of AuNPs and 5-FU causes an S phase increase with a G2/M decrease, but only in the case of the 30 and 15 nm NLS-AuNPs (Fig. 2A,B).

The cell cycle regulation observed for the combination of AuNPs and 5-FU suggests that the potency of 5-FU could be enhanced when administered after an initial 24 h treatment with the AuNPs tested in this work. In order to assess this potency, we have calculated the 5-FU efficacy by dividing the S phase population by the G2/M phase population. This value is justified as the chemosensitivity factor since 5-FU itself causes an S phase accumulation with a G2/M phase depletion (Fig. 2), and previous reports have defined the resistance to 5-FU as a decrease in S phase with an increase in G2/M phase populations.(17) Figure 3 shows the 5-FU chemosensitivity factors for the various nanoparticle treatments alone (0.4 nM, 24 h), as well as in combination with 100 μM 5-FU (48 h). The inherent 5-FU efficacy value for HSC-3 cells is around 1.6 and after treatment with 100 μM 5-FU, this value is increased to 5.8. In terms of the various nanoparticles tested here, the 30 nm NLS-AuNPs have the greatest impact on 5-FU efficacy, increasing the value to 21.4 and when combined with 100 μM 5-FU, the value is increased even more, to 29.8. The 15 nm NLS-AuNPs increase 5-FU efficacy to 2.5, and only up to 6.3 when combined with 5-FU. The 30 nm RGD-AuNPs increase 5-FU efficacy to 4.1, but only up to 6.9 when combined with 5-FU. It is clear here that 5-FU efficacy is influenced by gold nanoparticles and is dependent on the size and location of nanoparticles within cells, with 30 nm nuclear-localized AuNPs being the most effective at enhancing 5-FU efficacy.

Enhanced 5-Fluorouracil Chemosensitivity

Utilizing the various AuNPs and their ability to regulate the cell cycle, as shown above, we can now assess whether these nanoparticles actually sensitize HSC-3 cells to 5-FU treatment (*i.e.* chemosensitization). HSC-3 cells were initially treated with the different AuNPs (0.4 nM, 24 h) in order to allow for accumulation of cells in the S phase and depletion of cells in the G2/M phase. Following AuNP treatment, 5-FU was introduced at increasing concentrations (10–500 μM, 48 h) and the cell viability was determined. Figure 4 displays the results of the cell viability analysis, comparing between both AuNP size and AuNP surface functionalization (*i.e.* nanoparticle location within the cell). It should first be noted

that none of the AuNP formulations shown here are inherently cytotoxic to the HSC-3 cells (no significant reduction in cell viability upon 24 h treatment with 0.4 nM AuNPs), alleviating common toxicity issues presented with combination chemotherapies. As one would expect, cell viability decreases with increasing concentrations of 5-FU. The lowest cell viability observed for the control (no AuNPs) is about 40% when the cells are treated with 500 μM 5-FU, but when pre-treated with 30 nm NLS-AuNPs (Fig. 4A), the cell viability is significantly reduced to 17%. In addition to the 500 μM 5-FU treatment being more effective, concentrations as low as 100 μM are also significantly enhanced by the pre-treatment of cells with the 30 nm NLS-AuNPs (Fig. 4A). When comparing AuNP size, the 15 nm NLS-AuNPs (Fig. 4B) do not appear to enhance the efficacy of 5-FU at any of the 5-FU treatment concentrations tested. In particular, at 5-FU concentrations of 10 and 100 μM, the cell viability is significantly enhanced by pre-treatment of cells with 15 nm NLS-AuNPs. At increasing concentrations of 5-FU (200–500 μM), pre-treatment of cells with 15 nm NLS-AuNPs has no significant effect on 5-FU efficacy. Another comparison here is the different effects induced when the nanoparticles are localized in the cytoplasm of the cell (RGD-AuNPs) as opposed to localized at the nucleus of the cell (NLS-AuNPs). When cells are pre-treated with 30 nm RGD-AuNPs (Fig. 4C), the efficacy of 10 μM 5-FU is significantly enhanced (79% cell viability reduced to 43%). At higher 5-FU treatment concentrations (100–500 μM), the pre-treatment of cells with 30 nm RGD-AuNPs does not have any significant effect on 5-FU efficacy.

It is clear from the cell viability results shown in Figure 4 that there are definite differences in the 5-FU efficacy after cells are pre-treated with various AuNPs. The 30 nm NLS-AuNPs appear to be the most effective at sensitizing HSC-3 cells to 5-FU treatment, which is also confirmed by the high 5-FU efficacy values determined by cell cycle analysis (Fig. 3), and no apparent increase in 5-FU uptake by the presence of nanoparticles was observed in this case (see Supporting Information, Figure S1). Smaller AuNPs (15 nm NLS-AuNPs) and AuNPs localized at the cytoplasm (30 nm RGD-AuNPs) do not consistently enhance the efficacy of 5-FU, which is also confirmed by the lower 5-FU efficacy values determined by cell cycle analysis (Fig. 3).

In order to further assess the mode by which the 30 nm NLS-AuNPs chemosensitize HSC-3 cells to 5-FU, cell death was investigated by flow cytometry analysis of cells labeled with the nucleic acid dye, propidium iodide (necrotic cells), cells stained with a phosphatidylserine label, Annexin-V-FITC (early apoptotic cells), cells labeled with both (late apoptotic), and cells that are unlabeled (live cells). Figure 5 displays percentages of necrotic (red), late apoptotic (dark blue), early apoptotic (light blue) and live (green) cells after treatment with 0.4 nM 30 nm NLS-AuNPs alone (24 h), 150 μM 5-FU alone (48 h), as well as 150 μM 5-FU (48 h) after pre-treatment with 30 nm NLS-AuNPs (0.4 nM, 24 h). The primary mode of cell death upon treatment with 5-FU appears to be via early apoptosis. Interestingly, the 30 nm NLS-AuNP treatment also exhibits a higher degree of early apoptosis, compared to necrosis or late apoptosis. Although early apoptosis is the predominant mode of cell death, late apoptosis and necrosis also occur to a significant degree. In terms of late apoptosis, when cells are treated with the combination of 30 nm NLS-AuNPs (0.4 nM, 24 h) and 150 μM 5-FU (48 h), the population is significantly enhanced compared to either treatment alone. In terms of necrosis, the population is also

significantly enhanced for the combination treatment, compared to treatment with only 30 nm NLS-AuNPs or only 5-FU. In looking at the early apoptotic populations, which appear to be the dominant mode of cell death for both individual treatments, the pre-treatment with 30 nm NLS-AuNPs does not enhance the amount of early apoptotic cells. It is interesting to note that this is the only population of dead cells in which this trend is observed, possibly due to the fact that the 30 nm NLS-AuNPs alone induce a smaller population of early apoptotic cells than the 5-FU alone, therefore not providing any enhancement in this mode of cell death.

CONCLUSIONS

In conclusion, we have shown that nuclear-targeted gold nanoparticles (NLS-AuNPs), specifically 30 nm in diameter, regulate the cell cycle of HSC-3 cells by inducing an accumulation of cells in the S phase with a depletion of cells in the G2/M phase. The S phase accumulation and G2/M phase depletion can be used to quantify the efficacy of a common chemotherapeutic agent, 5-Fluorouracil (5-FU). Of all the nanoparticles tested in this work, the 5-FU efficacy value is highest when cells are treated with 30 nm NLS-AuNPs (0.4 nM, 24 h), compared with 15 nm NLS-AuNPs or 30 nm RGD-AuNPs (cytoplasm localized AuNPs). This high 5-FU efficacy value is further confirmed when testing the cytotoxicity of 5-FU after pre-treatment with the various AuNPs. The cell viability of 5-FU treated cells is significantly reduced when the cells are pre-treated with 30 nm NLS-AuNPs (0.4 nM, 24 h), compared with cells pre-treated with the smaller NLS-AuNPs or the RGD-AuNPs. More detailed analyses of the modes of cell death involved with 5-FU treatment revealed that these 30 nm NLS-AuNPs also enhance levels of late apoptosis and necrosis when introduced to the cells 24 h prior to 5-FU treatment. It is clear that cell cycle regulation plays a major role in enhancing drug efficacy in malignant cells. It has been previously demonstrated that gold nanoparticles are capable of altering the cell cycle via regulation of cyclins, cyclin-dependent kinases (CDKs),(23) and cell cycle inhibitor proteins (p21 and p27).(24) From the results shown here, it is indeed possible that our nuclear-targeted AuNPs are causing alterations in the expression of these cell cycle regulators, and elucidation of the detailed mechanism by which they are capable of doing this will be essential. Once the molecular mechanisms involved in AuNP-induced cell cycle alterations are determined, chemosensitization via AuNPs can be exploited as a new technique for the treatment of various cancers with various chemotherapies.

Supplementary Material

Refer to Web version on PubMed Central for supplementary material.

Acknowledgments

This work was supported by the National Institutes of Health National Cancer Institute under grant No. CNPP U01CA151802.

References

1. AshaRani PV, Low Kah Mun G, Hande MP, Valiyaveettil S. Cytotoxicity and genotoxicity of silver nanoparticles in human cells. ACS Nano. 2009; 3:279–290. [PubMed: 19236062]

2. Kang B, Mackey MA, El-Sayed MA. Nuclear targeting of gold nanoparticles in cancer cells induces DNA damage, causing cytokinesis arrest and apoptosis. J Am Chem Soc. 2010; 132:1517–1519. [PubMed: 20085324]
3. Austin LA, Kang B, Yen CW, El-Sayed MA. Nuclear targeted silver nanospheres perturb the cancer cell cycle differently than those of nanogold. Bioconjug Chem. 2011; 22:2324–2331. [PubMed: 22010874]
4. Mackey MA, Saira F, Mahmoud MA, El-Sayed MA. Inducing Cancer Cell Death by Targeting Its Nucleus: Solid Gold Nanospheres versus Hollow Gold Nanocages. Bioconjug Chem. 2013; 24:897–906. [PubMed: 23777334]
5. Hirsch LR, Stafford RJ, Bankson JA, Sershen SR, Rivera B, Price RE, Hazle JD, Halas NJ, West JL. Nanoshell-mediated near-infrared thermal therapy of tumors under magnetic resonance guidance. Proc Natl Acad Sci U S A. 2003; 100:13549–13554. [PubMed: 14597719]
6. O'Neal DP, Hirsch LR, Halas NJ, Payne JD, West JL. Photo-thermal tumor ablation in mice using near infrared-absorbing nanoparticles. Cancer Lett. 2004; 209:171–176. [PubMed: 15159019]
7. Huang X, El-Sayed IH, Qian W, El-Sayed MA. Cancer cell imaging and photothermal therapy in the near-infrared region by using gold nanorods. J Am Chem Soc. 2006; 128:2115–2120. [PubMed: 16464114]
8. El-Sayed IH, Huang X, El-Sayed MA. Selective laser photo-thermal therapy of epithelial carcinoma using anti-EGFR antibody conjugated gold nanoparticles. Cancer Lett. 2006; 239:129–135. [PubMed: 16198049]
9. Huang X, Jain PK, El-Sayed IH, El-Sayed MA. Gold nanoparticles: interesting optical properties and recent applications in cancer diagnostics and therapy. Nanomedicine (Lond). 2007; 2:681–693. [PubMed: 17976030]
10. Chen J, Wang D, Xi J, Au L, Siekkinen A, Warsen A, Li ZY, Zhang H, Xia Y, Li X. Immuno gold nanocages with tailored optical properties for targeted photothermal destruction of cancer cells. Nano Lett. 2007; 7:1318–1322. [PubMed: 17430005]
11. Dickerson EB, Dreaden EC, Huang X, El-Sayed IH, Chu H, Pushpanketh S, McDonald JF, El-Sayed MA. Gold nanorod assisted near-infrared plasmonic photothermal therapy (PPTT) of squamous cell carcinoma in mice. Cancer Lett. 2008; 269:57–66. [PubMed: 18541363]
12. Bhattacharya RMP, Xiong Z, Atala A, Soker S, Mukhopadhyay. Gold Nanoparticles Inhibit VEGF165-Induced Proliferation of HUVEC Cells. Nano Lett. 2004; 4:2479–2481.
13. Mukherjee P, Bhattacharya R, Wang P, Wang L, Basu S, Nagy JA, Atala A, Mukhopadhyay D, Soker S. Antiangiogenic properties of gold nanoparticles. Clin Cancer Res. 2005; 11:3530–3534. [PubMed: 15867256]
14. Roa W, Zhang X, Guo L, Shaw A, Hu X, Xiong Y, Gulavita S, Patel S, Sun X, Chen J, Moore R, Xing JZ. Gold nanoparticle sensitize radiotherapy of prostate cancer cells by regulation of the cell cycle. Nanotechnology. 2009; 20:375101. [PubMed: 19706948]
15. Xu W, Luo T, Li P, Zhou C, Cui D, Pang B, Ren Q, Fu S. RGD-conjugated gold nanorods induce radiosensitization in melanoma cancer cells by downregulating alpha(v)beta(3) expression. Int J Nanomedicine. 2012; 7:915–924. [PubMed: 22412298]
16. Longley DB, Harkin DP, Johnston PG. 5-fluorouracil: mechanisms of action and clinical strategies. Nat Rev Cancer. 2003; 3:330–338. [PubMed: 12724731]
17. De Angelis PM, Svendsrud DH, Kravik KL, Stokke T. Cellular response to 5-fluorouracil (5-FU) in 5-FU-resistant colon cancer cell lines during treatment and recovery. Mol Cancer. 2006; 5:20. [PubMed: 16709241]
18. Yoshiba S, Ito D, Nagumo T, Shirota T, Hatori M, Shintani S. Hypoxia induces resistance to 5-fluorouracil in oral cancer cells via G(1) phase cell cycle arrest. Oral Oncol. 2009; 45:109–115. [PubMed: 18710819]
19. Frens G. Controlled Nucleation for Regulation of Particle-Size in Monodisperse Gold Suspensions. Nature Phys Sci. 1973; 241:20–22.
20. Liu X, Atwater M, Wang J, Huo Q. Extinction coefficient of gold nanoparticles with different sizes and different capping ligands. Colloids Surf B Biointerfaces. 2007; 58:3–7. [PubMed: 16997536]

21. Andreadis C, Vahtsevanos K, Sidiras T, Thomaidis I, Antoniadis K, Mouratidou D. 5-Fluorouracil and cisplatin in the treatment of advanced oral cancer. Oral Oncol. 2003; 39:380–385. [PubMed: 12676258]

22. Yoshitomi I, Kawasaki G, Yanamoto S, Mizuno A. Orotate phosphoribosyl transferase mRNA expression in oral squamous cell carcinoma and its relationship with the dihydropyrimidine dehydrogenase expression and the clinical effect of 5-fluorouracil. Oral Oncol. 2006; 42:880–887. [PubMed: 16757204]

23. Roa W, Zhang XJ, Guo LH, Shaw A, Hu XY, Xiong YP, Gulavita S, Patel S, Sun XJ, Chen J, Moore R, Xing JZ. Gold nanoparticle sensitize radiotherapy of prostate cancer cells by regulation of the cell cycle. Nanotechnology. 2009; 20

24. Bhattacharya R, Patra CR, Verma R, Kumar S, Greipp PR, Mukherjee P. Gold nanoparticles inhibit the proliferation of multiple myeloma cells. Advanced materials. 2007; 19:711-+.

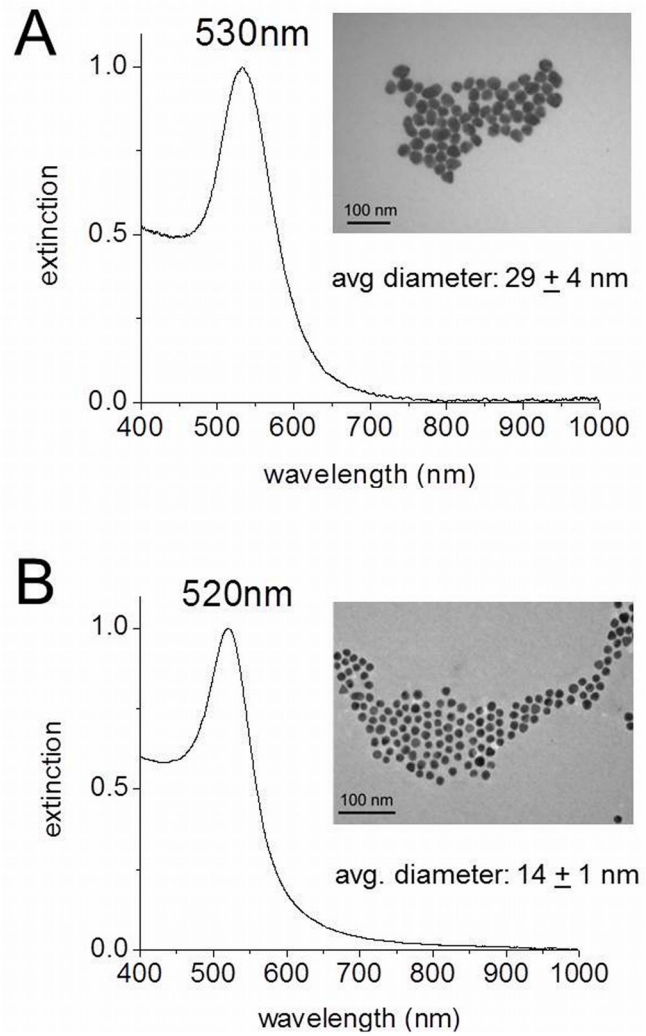

Figure 1.

UV-Vis spectra and TEM images (inset) of AuNPs synthesized via citrate reduction of $HAuCl_4$. (A) AuNPs with a surface plasmon resonance at 530 nm have a diameter of 29 ± 4 nm. (B) AuNPs with a surface plasmon resonance at 520 nm have a diameter of 14 ± 1 nm.

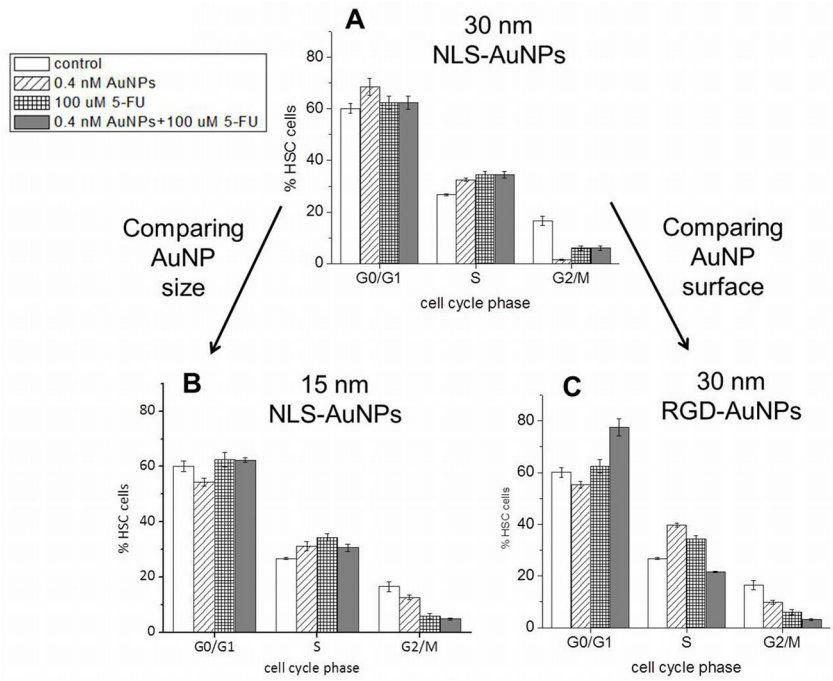

Figure 2.

Cell cycle analysis of HSC-3 cells after treatment with various AuNPs (0.4 nM, 24 h) and 5-FU (100 μM, 48 h); cells that were not treated (control), cells treated with AuNPs alone, cells treated with 5-FU alone, and cells treated with combination of AuNPs and 5-FU are shown. Comparison between AuNP size: (A) 30 nm NLS-AuNPs versus (B) 15 nm NLS-AuNPs. Comparison between AuNP surface functionalization: (A) 30 nm NLS-AuNPs versus (C) 30 nm RGD-AuNPs.

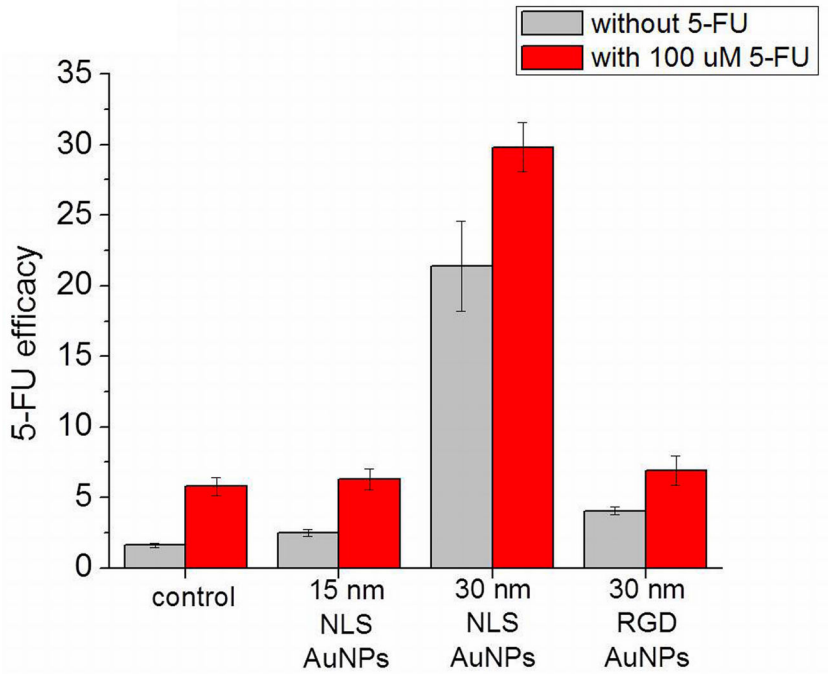

Figure 3.

5-FU efficacy in HSC-3 cells after treatment with various AuNPs (0.4 nM, 24 h) and 5-FU (100 μM, 48 h); control represents cells that were not treated with any AuNPs. Cells that were not treated with 5-FU, and cells that were treated with 5-FU are shown. 5-FU efficacy is defined as % cells in S phase divided by % cells in G2/M phase of the cell cycle.

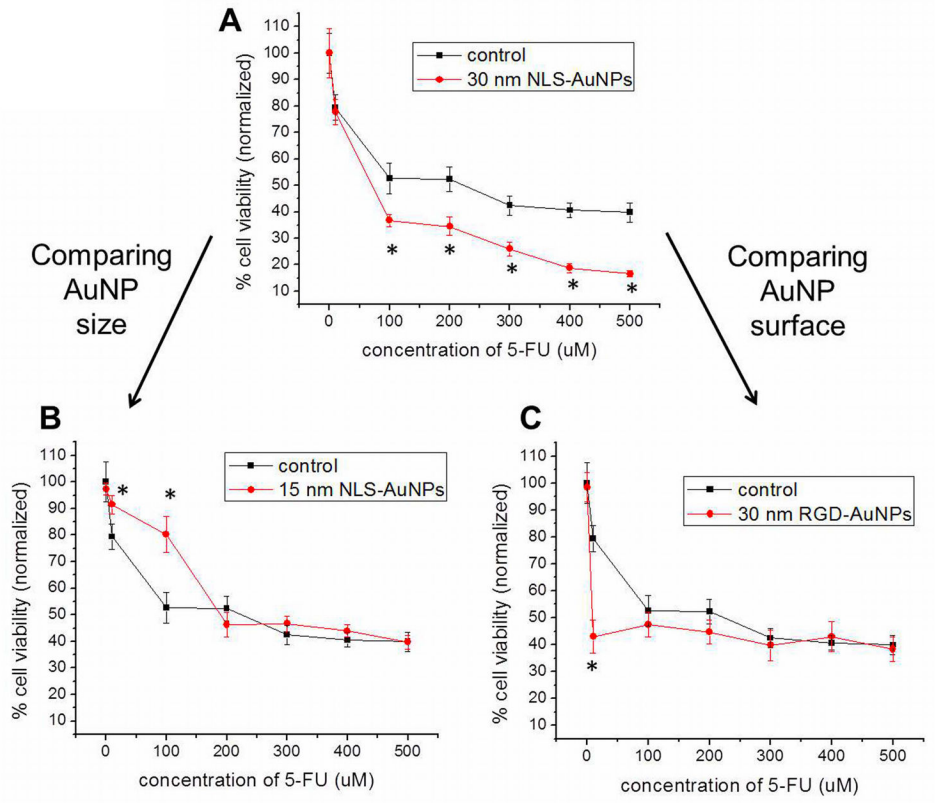

Figure 4.

Cell viability determined by an XTT assay of HSC-3 cells after treatment with various AuNPs (0.4 nM, 24 h) and 5-FU (10–500 μM, 48 h); c that were only treated with 5-FU (control, ■) and cells treated with a combination of AuNPs and 5-FU (●). Comparison between AuNP size: (A) 30 nm NLS-AuNPs versus (B) 15 nm NLS-AuNPs. Comparison between AuNP surface functionalization: (A) 30 nm NLS-AuNPs versus (C) 30 nm RGD-AuNPs. Statistical significance between cells treated with only 5-FU and cells treated with combination of AuNPs and 5-FU is indicated by * ($p < 0.05$).

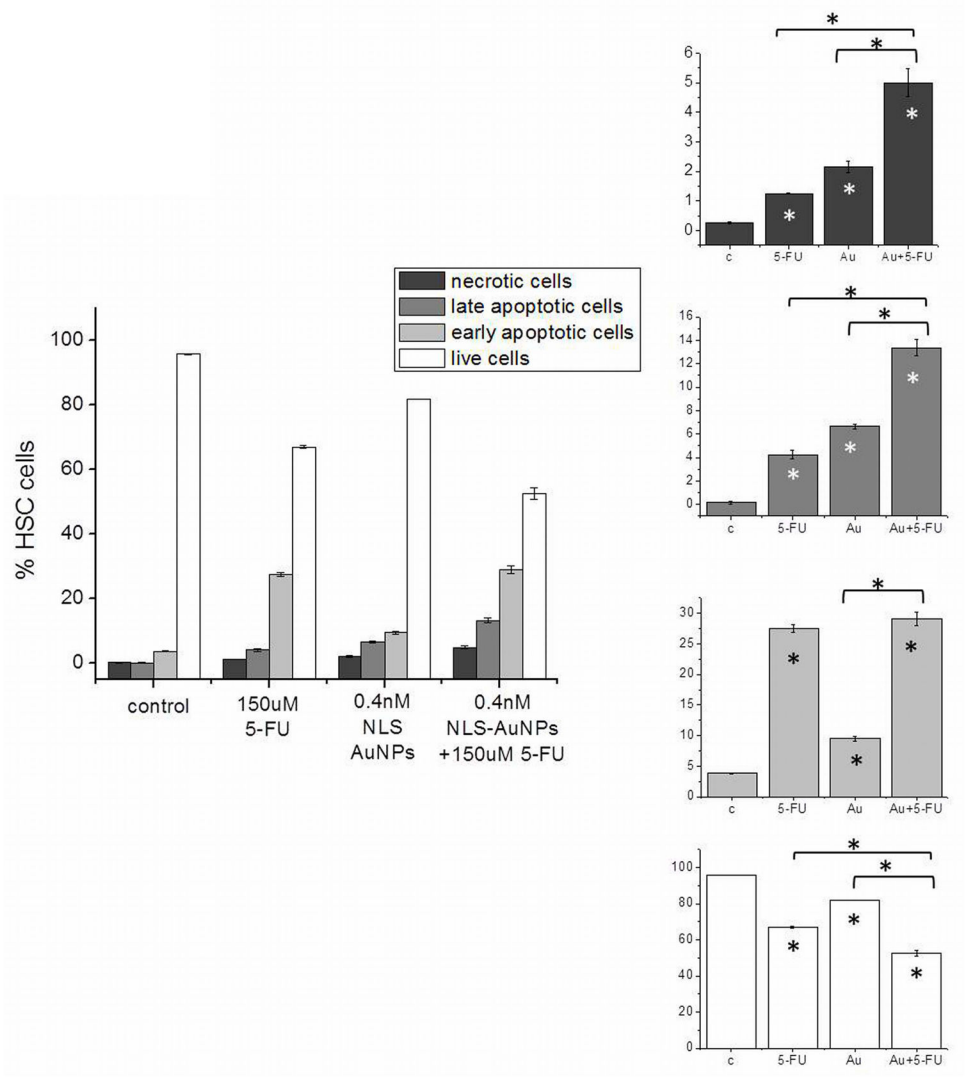

Figure 5.

Flow cytometry analysis of HSC-3 cell death after treatment with 0.4 nM NLS-AuNPs (24 h), 150 μM 5-FU (48 h) or 0.4 nM NLS-AuNPs (24 h) followed by 150 μM 5-FU (48 h). Right panel shows (top to bottom) necrotic populations, late apoptotic populations, early apoptotic populations, and live populations for cells that were untreated (c), treated with 150 μM 5-FU for 48 h (5-FU), treated with 0.4 nM 30 nm AuNPs for 24 h (Au) and treated with 150 μM 5-FU (48 h) after 24 h pre-treatment with 0.4 nM 30 nm NLS-AuNPs (Au + 5-FU). Statistical significance with respect to the control is indicated by * ($p < 0.05$) within the bars of the graph. Statistical significance with respect to different treatment groups indicated by * ($p < 0.05$) above graph.

Table 1

Dynamic light scattering measurements of the hydrodynamic diameter and zeta potential for various gold nanoparticles used in this study.

Nanoparticle Core Size (diameter)	Surface Functionalization	Hydrodynamic Diameter	Zeta Potential
15 nm	Citrate	22 nm	−33 mV
	PEG + NLS	58 nm	−4 mV
30 nm	Citrate	49 nm	−33 mV
	PEG + RGD	73 nm	6 mV
	PEG + NLS	87 nm	−3 mV